Characterization and modelling of the ion-irradiation induced disorder in 6H-SiC and 3C-SiC single crystals

A. Debelle, L. Thome, D Dompoint, Alexandre Boulle, F. Garrido, J. Jagielski, D. Chaussende

Characterization and modelling of the ion-irradiation induced disorder in 6H-SiC and 3C-SiC single crystals

A. Debelle[1*], L. Thomé[1], D. Dompoint[2], A. Boulle[2], F. Garrido[1], J. Jagielski[3], D. Chaussende[4],

[1]Centre de Spectrométrie Nucléaire et de Spectrométrie de Masse (CSNSM), CNRS-IN2P3-Univ. Paris-Sud, 91405 Orsay Cedex, France

[2]Science des Procédés Céramiques et de Traitements de Surface (SPCTS), CNRS UMR 6638, Centre Européen de la Céramique, 12 rue Atlantis, 87065 Limoges, France

[3]Institute for Electronic Materials Technology, Wolczynska 133, 01-919 Warsaw, Poland. The Andrzej Soltan Institute for Nuclear Studies, 05-400 Swierk/Otwock, Poland

[4]Laboratoire des Matériaux et du Génie Physique (LMGP), CNRS UMR 5628, Grenoble INP - Minatec, 3 parvis Louis Néel, BP 257, 38016 Grenoble Cedex 01, France

Abstract

6H-SiC and 3C-SiC single crystals were simultaneously irradiated at room temperature with 100-keV Fe ions at fluences up to $4x10^{13}$ cm^{-2} (~0.7 dpa), *i.e.* up to amorphization. The disordering behaviour of both polytypes has been investigated by means of Rutherford backscattering spectrometry in the channelling mode and synchrotron X-ray diffraction. For the first time, it is experimentally demonstrated that the general damage build-up is similar in both polytypes. At low dose, irradiation induces the formation of small interstitial-type defects. With increasing dose, amorphous domains start to form at the expense of the defective crystalline regions. Full amorphization of the irradiated layer is achieved at the same dose (~0.45 dpa) for both polytypes. It is also shown that the interstitial-type defects formed during the first irradiation stage induce a tensile elastic strain (up to ~3.8%) to which is associated an elastic energy. It is conjectured that this stored energy destabilizes the current defective microstructure observed at low dose and stimulates the formation of the amorphous nanostructures at higher dose. Finally, the disorder accumulation has been successfully reproduced with two models (namely MSDA and DI/DS). Results obtained from this modelling are compared and discussed in the light of experimental data.

PACS numbers: 61.80.Jh; 61.85.+p; 61.05.cp; 61.72.-y; 81.05.Je

* Author to whom correspondence should be addressed: aurelien.debelle@u-psud.fr

1. Introduction

Over the last decades, silicon carbide (SiC) has been attracting an increasing interest owing to many outstanding physical and chemical properties that make it a prominent candidate material for devices in extreme environments. For instance, in addition to high-temperature, high-power and high-frequency microelectronic and optoelectronic applications [for a review see Ref 1], SiC is also strongly envisioned in severe irradiation conditions such as structural components in fusion reactors [2] or cladding material for gas-cooled fission reactors [3]. To validate its use for these latter applications, a comprehensive understanding of its disordering behaviour under ion irradiation appears as a major fundamental issue.

Numerous polymorphs of SiC exist, but the hexagonal 4H-SiC and 6H-SiC are the most commonly available with a monocrystalline structure. Thus, computational [4-6] and extensive experimental [7-27] research works have been devoted to the study of radiation effects in these polytypes. On the contrary, due to the difficulty to elaborate high-quality single crystals, the cubic 3C-SiC polytype has been principally the focus of theoretical research efforts [4,7,28-36], with very few experimental studies [37-41]. Consequently, experimental data on irradiated 3C-SiC, which are yet mandatory to, e.g., refine analytical and phenomenological models, are lacking. In addition, only indirect (or incomplete) clues were provided on the comparison of the behaviour of cubic versus hexagonal polymorphs under ion irradiation [7,41].

The present paper reports the first direct comparison of the disorder build-up in 6H-SiC and 3C-SiC single crystals (SCs) simultaneously irradiated under the same conditions (namely 100-keV Fe at RT) to fluences up to amorphization. Two complementary analysis techniques, namely Rutherford backscattering spectrometry in the channelling mode (RBS/C) and X-ray diffraction (XRD), were used to monitor and characterize the irradiation-induced damage in both polytypes. Two physical models implementing a different approach of the amorphization process are used to reproduce the disorder build-up.

2. Experimental details

2.1. 6H-SiC and 3C-SiC single crystals

(0001)-oriented 6H-SiC and (001)-oriented 3C-SiC SCs, elaborated by Cree Research Inc. and HAST Corporation, respectively, were used for this study. It is worth emphasizing that they both exhibit a good crystalline quality. For instance, (i) the value of χ_{min}, which is the ratio, just below the surface peak, of the backscattering yield in the virgin spectrum to the yield in the random spectrum, was found to be equal to ~2% for both polytypes in the present study; (ii) the so-called 'rocking-curves' (XRD ω-scans) are very narrow, with a FWHM of less than 0.05°. The only difference between the two polytypes is that 3C-SiC SCs contain stacking faults in the {111} planes, as recently demonstrated by Boulle et al. [42]. These defects are visible on the reciprocal space map (RSM) displayed in Figure 1 through the presence of the diffuse streak labelled 'SF'. Note that this RSM has been recorded around the (004) reflection of the 3C-SiC SC irradiated at low dose (~0.07 dpa).

2.2. Irradiation and characterization

SCs were irradiated 7° off the major crystallographic direction **(**in order to avoid channelling effects) with 100-keV Fe ions at room temperature (RT). Several ion fluences have been used, ranging from $4x10^{13}$ up to $4x10^{14}$ cm^{-2}. The corresponding conversion factor for the displacements per atom (dpa) values at the damage peak is equal to ~$1.8x10^{-15}$ $dpa.cm^2$, as determined with SRIM calculations [43] using the recommended threshold displacement energies of 20 eV and 35 eV for the C and Si sublattices, respectively, for the two polytypes [28,33,36]. These values have shown to be the most relevant for the evaluation of the damage dose with the SRIM program. The ion flux was kept low (a few 10^{11} $cm^{-2}s^{-1}$) in order to avoid dose rate effects and significant temperature increase. The so-called median energy [44], $T_{1/2}$, of both Si and C primary knock-on atoms (PKAs) were determined from the weighted average recoil spectra [45] calculated from SRIM. This energy has shown to be a good representative to characterize the primary recoil energy spectrum with the resultant defect production. The corresponding values are ~3.7 keV and ~4.6 keV for Si and C PKAs, respectively.

RBS/C measurements were performed using a 1.4 MeV He^+ ion beam delivered by the ARAMIS accelerator of the JANNuS facility of the CSNSM-Orsay [46]. The energy resolution is ~ 12 keV. XRD experiments were carried out at the BM2 beamline [47] of the European Synchrotron Radiation Facility (ESRF, Grenoble, France). The wavelength of the X-ray beam was 0.148787 nm and the beam divergence, estimated from the peak width of an unirradiated crystal, was ~0.01°.

3. Results and discussion

3.1. Channelling analysis

Typical RBS/C spectra recorded on 6H-SiC and 3C-SiC SCs for selected Fe-ion fluences are displayed in Figure 2. Spectra obtained in both random (rotating crystal method) and aligned geometries are presented. For the sake of clarity, the signals corresponding to both C (starting below 400 keV) and Fe (located around 1000 keV) atoms have been omitted in the figure. It is worth noticing that RBS/C spectra recorded on 6H-SiC and 3C-SiC SCs are very similar. The spectra registered in a random direction display a plateau below 800 keV which arises from the backscattering of analyzing particles from the Si atoms of the crystals. The spectra registered in the main axis direction show (for both polytypes) a strong decrease of the backscattering yield due to the channelling effect, except in a thin layer close to the sample surface where the crystal is damaged by Fe irradiation. Actually, the bump clearly visible around 760 keV indicates the position of the maximum of the damage distribution (hereafter called R_D), which is ~35 nm in the current study. An increase with increasing ion fluence of the backscattering yield at R_D is observed for both polytypes. At a fluence of 2.5×10^{14} cm^{-2} (~0.45 dpa), the yield at R_D reaches the random level, indicating a full disorder, *i.e* amorphization of the irradiated part of crystals, as previously demonstrated in many studies [12,20,38-39]. It is worth noting that amorphization is achieved at the same fluence for both polytypes. This rather low critical dose for amorphization shows the high disordering susceptibility of both 6H-SiC and 3C-SiC upon elastic (nuclear) collisions; it corresponds to a cumulative deposited nuclear energy loss of ~29 eV/atom according to SRIM calculations. These results are in good agreement with

previous experimental observations in SiC irradiated under similar conditions, *i.e.* at RT in the hundred keV range (e.g. 500-keV N^+ [26] or 360-keV Ar^+ [38] ions). Above 2.5×10^{14} cm^{-2}, the amorphous region broadens and consumes the entire irradiated layer.

All RBS/C spectra were fitted (solid lines in Fig. 2) by using Monte-Carlo simulations performed with the McChasy computer code [48], which is a powerful and reliable tool competing favourably with standard analyses [49] for channelling data reduction. In particular, the comparison of the amount of irradiation-induced disorder can be safely estimated since the crystallographic arrangements in both SiC polytypes are explicitly included in the simulation. In this work, McChasy calculations rely on the basic assumption that a fraction f_D of (Si and C) atoms were randomly displaced from their original lattice site during irradiation. From these simulations, it is possible to determine the disorder depth profiles at each fluence, and then the damage build-up which is the variation of f_D at R_D with the irradiation fluence (or dose). The corresponding disorder-accumulation curves obtained for the Si sublattice for both SiC polymorphs are displayed in Figure 3. It appears that these curves are identical (except a weak difference in the low-fluence range). In a very recent study, Jiang *et al.* showed that irradiated 6H-SiC and 3C-SiC exhibit a very similar general damage build-up at low dose (up to 0.1 dpa) [41]; these authors suggested that this similar behaviour should be due to the fact that all the SiC polytypes present the same local structure based on the stacking of CSi_4 tetrahedrons. From the present results, it is clearly demonstrated that the general disorder accumulation is the same in both polytypes up to amorphization (at least under the current irradiation conditions). Besides, it exhibits the same nearly-sigmoidal dependence on irradiation dose.

3.2. XRD investigation

Figure 4 presents selected θ-2θ scans recorded on 6H-SiC and 3C-SiC SCs. First, it is important to note that, similarly to what was observed for RBS/C, the XRD curves corresponding to the two polymorphs exhibit the same features. In all the curves (*i.e.* for all fluences and for both polytypes), a sharp and intense signal is observed on the high-angle side. It corresponds to the scattering of the X-ray beam by the virgin part of the crystals underneath the damaged layer (since X-rays probe ~30 μm

in the present geometry). This signal is used as an internal strain gauge to quantify the irradiation-induced elastic strain. After irradiation, the XRD curves exhibit an additional signal coming from the damaged part of the crystals. This signal, located at lower 2θ angles, reveals an increase of the lattice parameter in the direction normal to the surface of the crystals. More precisely, a tensile elastic strain is measured up to 1.2×10^{14} cm^{-2} (~0.21 dpa). This increase of the lattice dimensions corroborates the results obtained by RBS/C for 2-MeV Au irradiated 6H-SiC [15]. The strain at this relatively low damage dose reaches a high level of ~3.8% in both polytypes. This positive strain can only be due to the formation of defects with a positive relaxation volume, which is the volume change of the crystal due to the distortion field of one defect. In the present case, only self-interstitial atoms (SIAs) created within displacement cascades can be invoked to explain the occurrence of this strain (the maximum Fe concentration is lower than 0.1 at.%). This finding confirms several computational works (principally Molecular Dynamics -MD- simulations) which showed that both Si and C interstitials, rather in the form of split interstitials (dumbbells), can be formed and remain stable at RT in SiC submitted to ion irradiation [20,30,33]. However, it is worth mentioning that many studies also provide clear experimental evidences of the formation of vacancy-like defects in SiC under ion irradiation [9,13,50]. Nevertheless, only interstitial defects can be detected in the present study. Indeed, RBS/C is weakly sensitive to vacancies, and even if both vacancies and interstitial are present, XRD is also more sensitive to interstitials since their relaxation volume is significantly larger than that of vacancies.

On the θ-2θ scans of the SCs irradiated at low fluence (4×10^{13} cm^{-2} - ~0.07 dpa), a fringe pattern is clearly visible. This feature is due to the presence of a non-homogeneous strain depth profile and arises from interferences between diffracted X-ray beams emerging from regions with the same strain level (see e.g. Refs. 51-53). Furthermore, on the corresponding RSM (see Figure 1), only a vertical streak (labelled 'D') coming from the damaged (irradiated) region of the crystals is observed. No broadening in the horizontal direction (equivalent to a rocking-curve) is measured as compared to that obtained from virgin crystals [42]. These observations demonstrate that the defects at the origin of the elastic strain are randomly distributed point defects or small defect clusters. Such a result is in good agreement with MD simulations [29,31-32,34] performed to simulate the displacement cascades

induced in SiC by Si and C PKAs with energies (in the keV range) similar to the $T_{1/2}$ values calculated for the current experiments. Actually, these MD calculations showed that, due to the short lifetime of the thermal spike and the dispersed structure of the collision cascades in SiC, the probability to form large defects is strongly reduced at low doses; in fact, very small defect clusters (containing up to maximum 4 atoms) are predominantly formed. The scattered intensity corresponding to the irradiated layer at high doses (from 1.6×10^{14} cm^{-2} - ~0.28 dpa) must be ascribed to diffuse scattering, and it is not anymore possible to define an elastic strain. Such a signal is consistent with a strongly defective crystalline lattice characterized by the presence of extended defects. Besides, this signal is located at low 2θ angles, which means that the irradiated layer is still characterized by an average lattice parameter which is larger than that of a virgin crystal. These observations clearly reveal a change in the nature of the defects above this dose, and they are consistent with the presence of amorphous clusters. This result is in agreement with MD simulations that showed, at high damage dose, the formation of such defective nanostructures due to defect-stimulated growth and coalescence of defect clusters. It is worth emphasizing that, at intermediate fluence (1.2×10^{14} cm^{-2} - ~0.21 dpa), XRD curves display a transitional shape exhibiting interference fringes superimposed on a broad diffuse signal. This remark suggests that, in this dose range, both small interstitial-type defects and amorphous clusters co-exist. This observation supports the assumption that amorphization in both 6H-SiC and 3C-SiC is not the result of a sudden collapse of the crystalline structure but rather a continuous process. This result corroborates the conclusion drawn by Grigull *et. al.* in 3C-SiC thin films irradiated with 360-keV Ar^{+} ions at low temperature [39].

3.3. Modelling of the damage build-up

Several phenomenological models were developed in recent years to account for the damage accumulation in irradiated materials. Two of them, namely Multi-Step Damage Accumulation (referred to as MSDA) [54] and Direct-Impact/Defect-Stimulated (referred to as DI/DS) [16,55] are particularly well adapted to describe the damage build-up observed in SiC irradiated with low-energy ions which mainly slow down *via* elastic (nuclear) collisions.

The MSDA model is based on the main assumption that the production of damage results from a series of successive atomic rearrangements (called steps) triggered by either microscopic or macroscopic processes. Each new step takes place when the material is destabilized by radiation damage, so that the new structure formed has a lower free energy than the previous one. Such processes are controlled by the probability that each incident ion hits an unmodified volume of the material, so that it can be described in the framework of a direct-impact mechanism. According to the above hypotheses, the equation which accounts for the multi-step transformation process may be written [54]:

$$f_D = \sum_{i=1}^{n} (f_{D,i}^{sat} - f_{D,i-1}^{sat})\, G\left[1 - \exp(-\sigma_i(\Phi - \Phi_{i-1}))\right] \qquad (1)$$

where n is the number of steps required for the achievement of the total process, Φ is the irradiation fluence (or the equivalent dose in dpa), $f_{D,i}^{sat}$ is the level of damage at saturation, σ_i is the cross-section for damage formation and Φ_i is the threshold fluence, for the i^{th} step. G is a function which transforms negative values into 0 and leaves positive values unchanged.

RBS/C data obtained in this work on both 6H-SiC and 3C-SiC SCs are nicely fitted in the framework of the MSDA model (see the dashed line in Fig. 3). The corresponding fitting parameters are listed in Table I. The value of n was found to be equal to 2, indicating that the damage build-up occurs in two steps. According to XRD results, the first step is likely due to the formation of small interstitial-type defects or defect clusters, leading to a disorder level at saturation $f_{D,1}^{sat} = 0.32$, as measured by RBS/C. This latter value is close to that determined for 6H-SiC irradiated at RT with

700-keV I ions ($f_{D,1}^{sat}$ = 0.27) [23] and to that obtained in the case of another amorphizable nuclear material, $Gd_2Ti_2O_7$, irradiated at RT with 4-MeV Au ions for which $f_{D,1}^{sat}$ = 0.24 [56]. It seems that the defects formed during the first irradiation step have a strong impact on the crystalline structure destabilization (higher damage and strain levels) of amorphizable materials. This property may explain the rapid occurrence of the second step in the damage build-up. Indeed, the transition fluence, Φ_2, arises at a fraction of dpa: (i) ~0.18 dpa in the current study, (ii) ~0.13 dpa for 6H-SiC irradiated at RT with 700-keV I ions and (iii) ~0.1 dpa for $Gd_2Ti_2O_7$ irradiated at RT with 4-MeV Au ions. This fluence threshold provides an indication of the stability of the materials upon irradiation. In the present work, according to XRD data, the second step is ascribed to the formation of a new type of defects (namely amorphous nanoclusters), which leads to full amorphization of the irradiated layer. The corresponding cross-section (30 dpa^{-1}) is about four times that of step 1 (8 dpa^{-1}). The physical relevance of the damage cross-sections σ_i is not straightforward for low-energy irradiation. Nevertheless, by analogy with the case of swift heavy ion irradiation, this parameter can be understood as the spatial extension over which the material is transformed during the impact of one incident ion. Consequently, higher values of σ_2 mean that the volume transformed by each incident ion in step 2 (formation of amorphous zones) is much larger than that in step 1 where interstitial clusters are created.

The damage build-up shown in Figure 3 may also be accounted for with the DI/DS model [16,55], which considers that f_D consists of contributions from amorphized and damaged-crystalline regions according to the relationship: $f_D = f_a + f_c$, where f_a is the amorphous fraction and f_c is the damaged fraction due to irradiation-induced point defects and small defect clusters in the remaining crystalline regions. In this description, f_a is represented by the direct-impact, defect-stimulated (DI/DS) model, which has proven to be consistent with RBS/C data in the case of SiC [5,16,19-20,26], according to the equation:

$$f_a = 1 - (\sigma_a + \sigma_s) / \left\{ \sigma_s + \sigma_a \exp\left[(\sigma_a + \sigma_s) \Phi \right] \right\} \quad (2)$$

(where σ_a is the cross-section for direct amorphization, σ_s is the effective cross-section for defect-stimulated amorphization, and Φ is the irradiation fluence (or the equivalent dose in dpa). The damage fraction f_c is usually reproduced by a simple defect accumulation model:

$$f_c = f_c^{sat}\left[1-\exp\left(-B\Phi\right)\right]\left(1-f_a\right) \quad (3)$$

where f_c^{sat} is the saturation value for the defect-induced disorder, and B is an effective recombination volume for the defects giving rise to f_c.

RBS/C data obtained on both 6H-SiC and 3C-SiC SCs irradiated with Fe ions are also well reproduced using equations (2) and (3) (see the solid line in Fig. 3). The corresponding fitting parameters are listed in Table II. No clear interpretation exists up to now about the significance of B. It can only be mentioned that the value found in this work lies in the range of those obtained in other studies [19-20,26]. Regarding f_c, it is first worth mentioning that its meaning relies on the assumption that its contribution to the total disorder arises from the accumulation of defects in the form of point defects or small clusters. This assumption is, as previously demonstrated by XRD, valid in the current study. As already observed in SiC [19-20,26], f_c is the primary contribution to the total disorder at low doses (here, up to ~0.1 dpa). Its value at saturation (f_c^{sat}~0.11) is much larger than that (f_c^{sat}~0.025) obtained in SiC irradiated with 2 MeV Au ions at RT [20]. This difference is consistent with MD calculations which demonstrated that increasing the mass of the incident particle (from Si to Au) leads to the formation of denser collision cascades, and therefore to a higher probability to form large defect clusters. Consequently, the dose range where f_c dominates (*i.e.* in the regime of creation of small defects) is reduced. The current f_c^{sat} value is on the contrary very close to the values derived after irradiation under similar conditions as those used in the present work, e.g. 500-keV N^+ irradiation [26], or 360-keV Ar^+ irradiation [38] (note that in this latter case the damage build-up is very similar to that obtained in the present study but it was unfortunately fitted with a double-cascade overlap model). As expected from previous works on SiC, the contribution of f_a to the total disorder early exceeds that of f_c. According to MD simulations, this transition occurs when collision cascades start to overlap previously damaged regions [34] (it is worth reminding that, in the framework of the MSDA model,

this transition occurs when the defective structure containing defect clusters becomes energetically unstable). In addition, σ_s is significantly larger than σ_a, this latter parameter being very small, as already reported in previous studies [16,19-20,26]. These observations indicate that (i) the probability of direct amorphization is very low, consistently with MD simulations [29,31-32,34], and (ii) defect-stimulated amorphization is the dominant mechanism in SiC. These results explain why only a small dose is required to achieve full amorphization. The presence of defective regions formed during the regime where f_c is the main contribution to f_d is the key parameter to explain the stimulation effect assumed in the DI/DS model.

It is worth emphasizing from Figure 3 that both MSDA and DI/DS models reproduce experimental data with a good accuracy. Actually, although they implement a different approach regarding the first stage of the damage build-up, they provide a similar description of the overall amorphization process. In the framework of the DI/DS model, it is assumed that defect clusters as well as amorphous clusters are formed from the very beginning of the disordering build-up, the cross-section for direct amorphization being very weak (0.08 dpa^{-1}). In the MSDA model, only small defect clusters are assumed to be created in the first step, *i.e.* up to a dose threshold of 0.18 dpa, with a much higher corresponding cross-section (8 dpa^{-1}). More work is needed (particularly a thorough examination by TEM of the crystals irradiated at ~0.14 dpa, *i.e.* just before the rapid increase of the damage fraction, see Fig. 3) to discriminate between the two representations. With increasing dose, the defect-stimulated amorphization process becomes predominant in the DI/DS model, and the corresponding cross-section is large (30 dpa^{-1}). A similar interpretation holds with the MSDA description, which is strengthened by the fact that the cross-section corresponding to the second step of damage accumulation is equal to that derived from the DI/DS model. Finally, using both representations it may be conjectured that the large elastic energy associated to the presence of radiation-induced defect clusters could be considered as a driving force that accelerates the destabilization of the defective structure observed at low dose and stimulates the formation of a new defect structure, as it was previously suggested in ion-irradiated YSZ [48,57-58].

4. Conclusion

The disordering behaviour, up to amorphization, of both 6H-SiC and 3C-SiC polytypes simultaneously irradiated at RT with low-energy ions has been investigated by means of two complementary techniques, namely RBS/C and XRD. Results demonstrate that the damage build-up exhibits the same nearly-sigmoidal dependence on dose in both polytypes. The disorder accumulation (sensed by RBS/C) has been successfully reproduced with two phenomenological models that provide a similar general description of the overall amorphization process consistent with the reported XRD data. In the low dose range (up to ~0.2 dpa), small interstitial-type defect(s) (clusters) are formed and induce the development of a tensile elastic strain to which is associated an elastic energy. With increasing dose, this strain increases (up to ~3.8%) and it is conjectured that it destabilizes the current structure of the materials. Amorphous domains thus start to form at the expense of the defective crystalline regions, and the cross-section for their formation is very large compared to that determined for the primary defects. It is proposed that the elastic energy associated to the SIA clusters may play an important role in this process. Finally, full amorphization of the irradiated layer is achieved at the same low dose (~0.45 dpa) for both polytypes.

Acknowledgements

Authors would like to thank M. Drouet (PPrime Institute – Poitiers) for the Fe irradiations. One of the authors (AD) is also indebted to Peter Rozsa for his help in the calculation of PKA median energies.

TABLES

Table I: Model parameters from fits of equation (1) to the experimental RBS/C data displayed in Figure 3. Note that the values of σ_1, σ_2 and Φ_2 are expressed in dpa units.

MSDA	n	f_{D1}^{sat}	σ_1 (dpa^{-1})	Φ_2 (dpa)	f_{D2}^{sat}	σ_2 (dpa^{-1})
	2	0.32 ± 0.07	8.0 ± 2.5	0.18 ± 0.06	1	30 ± 5

Table II: Model parameters from fits of equations (2) and (3) to the experimental RBS/C data displayed in Figure 3. Note that the values of σ_a, σ_s and B are expressed in dpa units.

DI/DS	σ_a (dpa^{-1})	σ_s (dpa^{-1})	B (dpa^{-1})	f_c^{sat}
	0.08 ± 0.02	30 ± 3	30 ± 18	0.11 ± 0.06

FIGURE CAPTIONS

Figure 1: Reciprocal space map recorded in the vicinity of the (004) reflection of 3C-SiC. The streaks labelled 'SF' (dotted lines) are due to stacking faults lying in the {111} planes. The streak labelled 'D' (dashed line) is due to the damaged layer of the crystal. The scale bar is 0.1 nm^{-1}.

Figure 2: RBS spectra (Si signal) recorded in random (stars) and axial (other symbols) orientations on (a) 6H-SiC and (b) 3C-SiC SCs before and after irradiation at RT with 100-keV Fe ions at increasing fluences. Energy of analyzing $^4He^+$ beam: 1.4 MeV. Lines are fits to data using the McChasy Monte-Carlo simulation code [48].

Figure 3: Accumulated damage at the maximum of the f_D depth distribution as a function of the ion fluence (and number of dpa) in 6H-SiC (circles) and 3C-SiC (squares) SCs irradiated with 100 keV Fe ions at RT. Solid and dashed lines are fits to the data with the DI/DS and MSDA models, respectively.

Figure 4: θ-2θ scans recorded in the vicinity of the (0012) reflection of (a) 6H-SiC and (b) (004) reflection of 3C-SiC. Labels correspond to the ion fluences (expressed in cm^{-2}). The X-ray wavelength is λ = 0.148787 nm. The upper axis indicates the elastic strain in the direction normal to the surface. Curves are shifted vertically for visualization purposes.

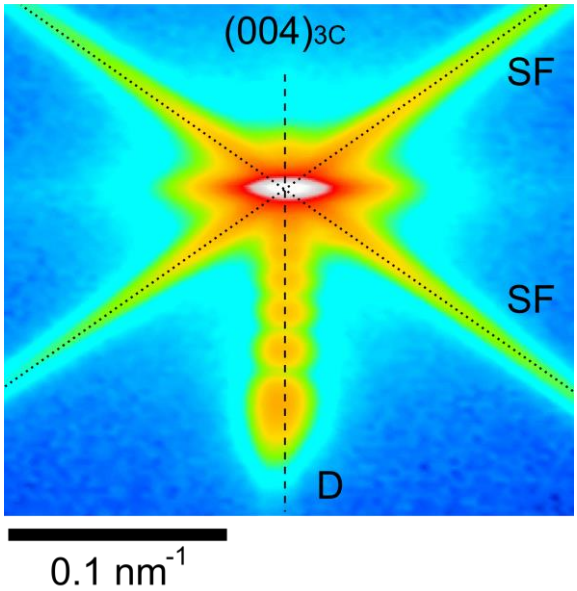

Figure 1

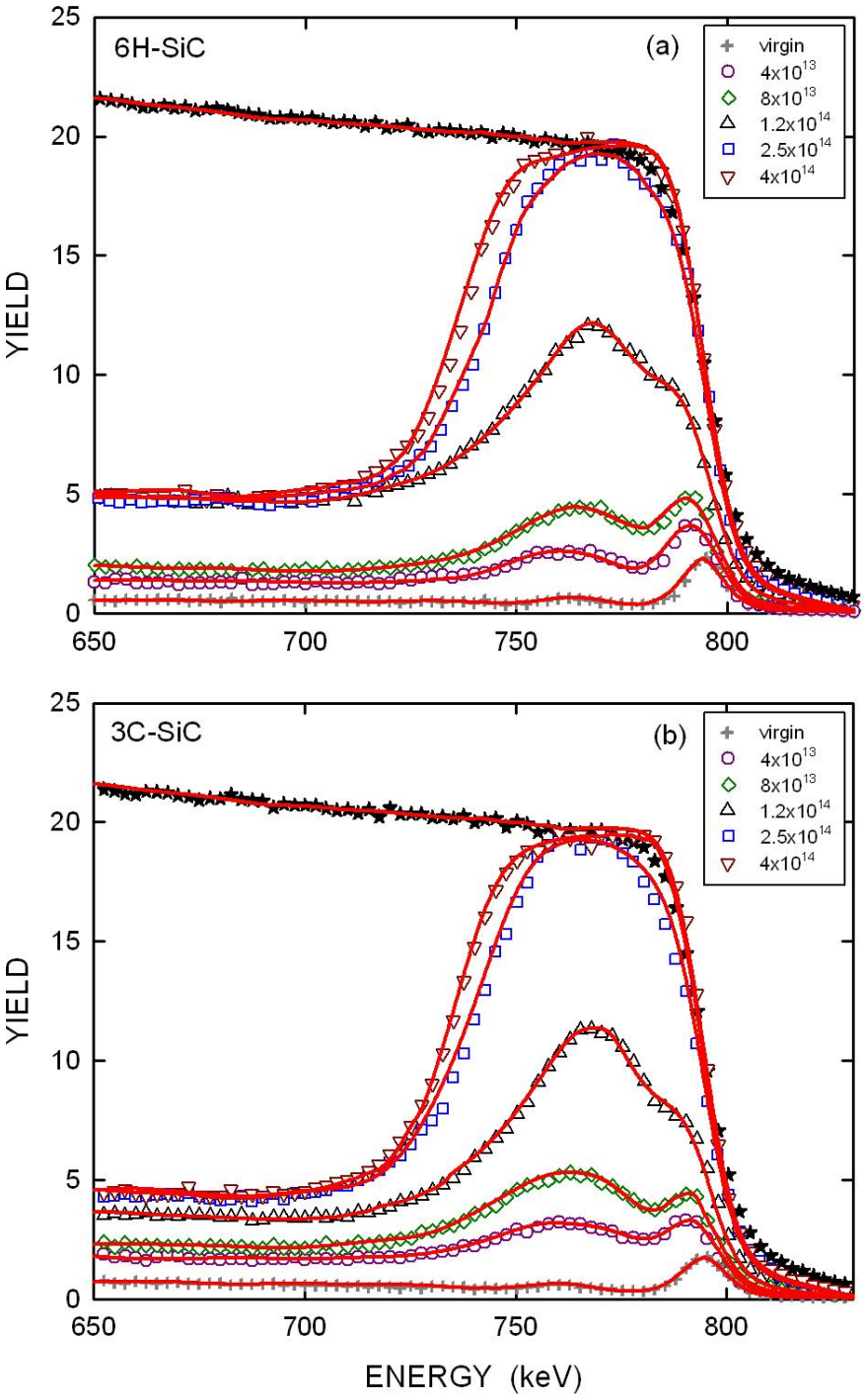
6H-SiC
(a)
virgin
4x10^13
8x10^13
1.2x10^14
2.5x10^14
4x10^14
YIELD
25
20
15
10
5
0
650
700
750
800
3C-SiC
(b)
virgin
4x10^13
8x10^13
1.2x10^14
2.5x10^14
4x10^14
YIELD
25
20
15
10
5
0
650
700
750
800
ENERGY (keV)

Figure 2

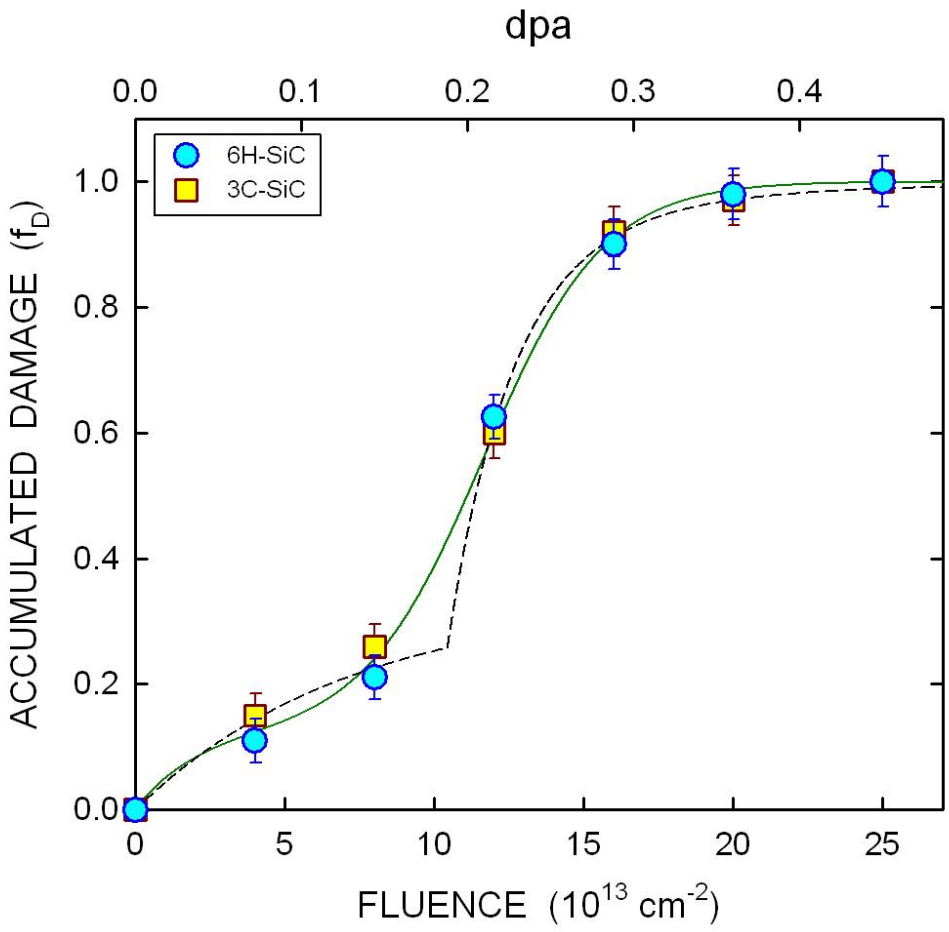
dpa
0.0
0.1
0.2
0.3
0.4
6H-SiC
3C-SiC
ACCUMULATED DAMAGE (f_D)
1.0
0.8
0.6
0.4
0.2
0.0
0
5
10
15
20
25
FLUENCE (10^13 cm^-2)

Figure 3

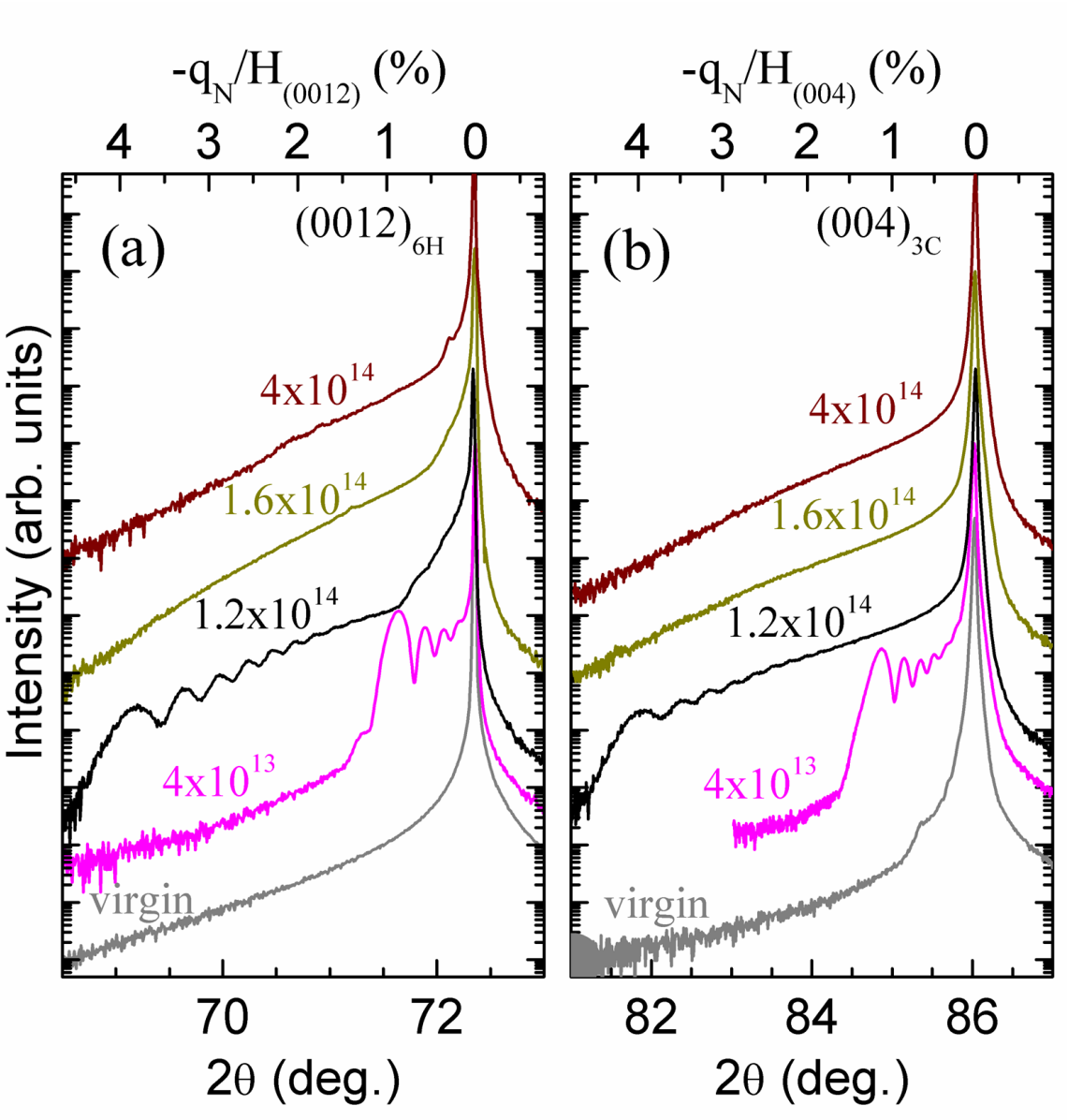
-q_N/H_(0012) (%)
4 3 2 1 0
(a)
(0012)_6H
4x10^14
1.6x10^14
1.2x10^14
4x10^13
virgin
Intensity (arb. units)
70 72
2θ (deg.)
-q_N/H_(004) (%)
4 3 2 1 0
(b)
(004)_3C
4x10^14
1.6x10^14
1.2x10^14
4x10^13
virgin
82 84 86
2θ (deg.)

Figure 4

REFERENCES

[1] C. Raynaud, J. Non-Cryst. Solids **280**, 1 (2001).

[2] A. Hasegawa, A. Kohyama, R.H. Jonec, L.L. Snead, B. Riccardi, P. Fenici, J. Nucl. Mater. **283**, 128 (2000).

[3] L.L. Snead, T. Nozawa, Y. Katoh, T.-S. Byun, S. Kondo, D.A. Petti, J. Nucl. Mater. **371**, 329 (2007).

[4] G. Brauer, W. Anwand, E.-M. Nicht, J. Kuriplach, M. Šob, N. Wagner, P. G. Coleman, M.J. Puska, and T. Korhonen, Phys. Rev. B **54**, 2512 (1996).

[5] Y. Zhang, F. Gao, W. Jiang, D. E. McCready, and W. J. Weber, Phys. Rev. B **70**, 125203 (2004).

[6] J.-P. Crocombette, G. Dumazer, N. Q. Hoang, F. Gao, and W. J. Weber, J. Appl. Phys. **101**, 023527-5 (2007).

[7] L.L. Snead and S.J. Zinkle, in Microstructure of Irradiated Materials, MRS Symp. Proc. vol. 373, eds. I.M. Robertson et al. (Mater. Res. Sot., Pittsburgh, 1995) p. 377.

[8] S. Dannefaer, D. Craigen, and D. Kerr, Phys. Rev. B **51**, 1928 (1995).

[9] G. Brauer, W. Anwand, P. G. Coleman, A. P. Knights, F. Plazaola, Y. Pacaud, W. Skorupa, J. Störmer, and P. Willutzki, Phys. Rev. B **54**, 3084 (1996).

[10] R. Nipoti, E. Albertazzi, M. Bianconi, R. Lotti, G. Lulli, M. Cervera, and A. Carnera, Appl. Phys. Letters **70**, 3425-3427 (1997).

[11] E. Wendler, A. Heft, and W. Wesch, Nucl. Instr. and Meth. B **141**, 105 (1998).

[12] L. L. Snead, S. J. Zinkle, J. C. Hay, and M. C. Osborne, Nucl. Instr. and Meth. B **141**, 123 (1998).

[13] M. F. Barthe, L. Henry, C. Corbel, G. Blondiaux, K. Saarinen, P. Hautojärvi, E. Hugonnard, L. Di Cioccio, F. Letertre, and B. Ghyselen, Phys. Rev. B **62**, 16638 (2000).

[14] E. Wendler and G. Peiter, J. Appl. Phys. **87**, 7679 (2000).

[15] W. Jiang and W. J. Weber, Phys. Rev. B **64**, 125206 (2001).

[16] Y. Zhang, W. J. Weber, W. Jiang, A. Hallen, and G. Possnert, J. Appl. Phys. **91**, 6388 (2002).

[17] A. A. Rempel, W. Sprengel, K. Blaurock, K. J. Reichle, J. Major, and H. E. Schaefer, Phys. Rev. Letters **89**, 185501 (2002).

[18] S. Muto and T. Tanabe, J. Appl. Phys. **93**, 3765 (2003).

[19] Y. Zhang, W. J. Weber, W. Jiang, C. M. Wang, V. Shutthanandan, and A. Hallen, J. Appl. Phys. **95**, 4012 (2004).

[20] W. Jiang, Y. Zhang, and W. J. Weber, Phys. Rev. B **70**, 165208 (2004).

[21] A. Kinomura, A. Chayahara, Y. Mokuno, N. Tsubouchi, and Y. Horino, J. Appl. Phys. **97**, 103538-6 (2005).

[22] S. Leclerc, A. Declemy, M. F. Beaufort, C. Tromas, and J. F. Barbot, J. Appl. Phys. **98**, 113506-6 (2005).

[23] A. Benyagoub, A. Audren, L. Thomé, and F. Garrido, Appl. Phys. Letters **89**, 241914-3 (2006).

[24] S. Yamazaki, K. Yamaya, M. Imai, and T. Yano, J. Nucl. Mater. **367-370**, 692 (2007).

[25] W. Jiang, P. Nachimuthu, W. J. Weber, and L. Ginzbursky, Appl. Phys. Letters **91**, 091918-3 (2007).

[26] Z. Zolnai, A. Ster, N. Q. Khanh, G. Battistig, T. Lohner, J. Gyulai, E. Kotai, and M. Posselt, J. Appl. Phys. **101**, 023502-11 (2007).

[27] X. Kerbiriou, J.-M. Costantini, M. Sauzay, S. Sorieul, L. Thomé, J. Jagielski, and J.-J. Grob, J. Appl. Phys. **105**, 073513-11 (2009).

[28] R. Devanathan and W. J. Weber, J. Nucl. Mater. **278**, 258 (2000).

[29] F. Gao and W. J. Weber, Phys. Rev. B **63**, 054101 (2000).

[30] F. Gao, E. J. Bylaska, W. J. Weber, and L. R. Corrales, Phys. Rev. B **64**, 245208 (2001).

[31] F. Gao and W. J. Weber, J. Appl. Phys. **89**, 4275 (2001).

[32] R. Devanathan, W. J. Weber, and F. Gao, J. Appl. Phys. **90**, 2303 (2001).

[33] L. Malerba and J. M. Perlado, Phys. Rev. B **65**, 045202 (2002).

[34] F. Gao and W. J. Weber, Phys. Rev. B **66**, 024106 (2002).

[35] F. Gao and W. J. Weber, Phys. Rev. B **69**, 224108 (2004).

[36] G. Lucas and L. Pizzagalli, Phys. Rev. B **72**, 161202 (2005).

[37] H. Inui, H. Mori, A. Suzuki, and H. Fujita, Phil. Mag. B **65**, 1 (1992).

[38] W. J. Weber, N. Yu, and L. M. Wang, J. Nucl. Mater. **253**, 53 (1998).

[39] S. Grigull, M. Ishimaru, M. Nastasi, C. A. Zorman, and M. Mehregany, Phil. Mag. Letters **81**, 55 (2001).

[40] Y. Katoh, N. Hashimoto, S. Kondo, L. L. Snead, and A. Kohyama, J. Nucl. Mater. **351**, 228 (2006).

[41] W. Jiang, W. J. Weber, J. Lian, and N. M. Kalkhoran, J. Appl. Phys. **105**, 013529-6 (2009).

[42] A. Boulle, D. Chaussende, L. Latu-Romain, F. Conchon, O. Masson, and R. Guinebretière, Appl. Phys. Lett. **89**, 091902 (2006).

[43] Ziegler J F, Biersack J P and Littmark U 1985 The Stopping Range of Ions in Solids vol 1 ed J F Ziegler et al (New York: Pergamon). SRIM program can be downloaded at: www.srim.org.

[44] The median energy $T_{1/2}$ is the value of T for which half of the defects are produced in cascades with energies greater than $T_{1/2}$, and half in cascades with energies less than $T_{1/2}$.

[45] R.S. Averback, J. Nucl. Mater. **216**, 49 (1994).

[46] Y. Serruys, M.-O. Ruault, P. Trocellier, S. Henry, O. Kaïtasov, and Ph. Trouslard, Nucl. Instr. and Meth. B **240**, 124 (2005).

[47] J.-L. Ferrer, J.-P. Simon, J.-F. Bérar, B. Caillot, E. Fanchon, O. Kaïkati, S. Arnaud, M. Guidotti, M. Pirocchi and M. Roth, J. Synchr. Rad. **5**, 1346 (1998).

[48] L. Nowicki, A. Turos, R. Ratajczak, A. Stonert and F. Garrido, Nucl. Instrum. Meth. B **240**, 277 (2005).

[49] Materials Analysis by Ion Channeling, ed. L.C. Feldman, J.W. Mayer and S.T. Picraux, Academic Press, New York (1982).

[50] A. Gentils, M.-F. Barthe, L. Thomé, and M. Behar, Appl. Surf. Science **255**, 78 (2008).

[51] A. Boulle, F. Conchon, and R. Guinebretière, J. Appl. Cryst. **42**, 85 (2009).

[52] A. Boulle and A. Debelle, J. Appl. Cryst., *accepted*.

[53] T. Emoto, J. Ghatak, P. V. Satyam, and K. Akimoto, J. Appl. Phys. **106**, 043516 (2009).

[54] J. Jagielski and L. Thomé, Appl Phys A **97** (2009) 147.

[55] W. J. Weber, Nucl. Instr. and Meth. B **166-167**, 98 (2000).

[56] G. Sattonnay, S. Moll, L. Thomé, C. Pascanut-Decorse, C. Legros, P. Simon, J. Jagielski, I. Jozwik and I. Monnet, *submitted to Phys. Rev. B.*

[57] S. Moll, L. Thomé, G. Sattonnay, A. Debelle, L. Vincent, F. Garrido, J. Jagielski, J. Appl. Phys. **106**, 073509 (2009).

[58] A. Debelle, S. Moll, B. Décamps, L. Thomé, G. Sattonnay, F. Garrido, I. Jozwik, J. Jagielski, Scripta Mater **63**, 665 (2010).